COBEM 2023 27TH INTERNATIONAL CONGRESS OF MECHANICAL ENGENEERING

ABCM Brazilian Society of Mechanical Sciences and Engineering
27th ABCM International Congress of Mechanical Engineering
December 04-08, 2023, Florianópolis-SC, Brazil

COB-2023-XXXX (XXXX is the identification number of the final paper) Improving Accuracy with Isogeometric Boundary Element Method (IGABEM): Applications in Potential Theory and Linear Elasticity

Deborah C. Nardi
Edson Denner Leonel
University of São Paulo - São Carlos School of Engineering - Department of Structural Engineering
deborahnardi@usp.br, edleonel@sc.usp.br

Abstract. *It is widely recognized that in recent years, there has been an increasing emphasis on enhancing the precision of numerical methods. One crucial aspect is the treatment of the geometry and mechanical field approximations of a problem within a numerical method since the accuracy of the solution depends on how well these aspects are treated. In this sense, the Isogeometric approach (IGA) is a relatively new computational method that aims to improve accuracy by directly linking Computer-Aided Design (CAD) software with numerical methods. IGA achieves this by using the same basis functions to represent both the geometry and the solution. By employing non-uniform rational B-splines (NURBS), IGA provides an accurate and efficient method for describing complex geometries. The conventional Boundary Element Method (BEM) uses Lagrangian polynomials to generate the shape and the basis functions of the problem under analysis. If NURBS are used instead of Lagrangian polynomials, the Isogeometric Boundary Element Method (IGABEM) is formed, offering precise geometry representation and improved accuracy in comparison to conventional BEM. This paper presents the IGABEM formulation and its application in solving potential and elastotastic problems. Numerical examples are included to compare the performance of conventional BEM and IGABEM.*

Keywords: *BEM, IGABEM, potential theory, linear elasticity.*

1. INTRODUCTION

Numerical approximations are often necessary for solving a wide range of physical and engineering problems. The most effective approach for solving boundary integral equations is the Boundary Element Method (BEM). This method proves particularly useful for addressing various problem types, including the potential theory and linear elasticity, which can be mathematically described in terms of integral equations.

The potential theory can be seen as a framework for understanding a specific differential equation known as Laplace's equation. This differential equation plays a fundamental role in various fields, describing phenomena such as steady heat flow in homogeneous media, steady fluid flow in ideal conditions, steady electric currents, and the equilibrium of elastic solids (Kellogg, 1953). The characteristics of a physical field can be effectively described using a scalar or vector potential function. In the context of BEM, this principle is applied by representing the physical field as a potential that satisfies either the Laplace or the Poisson equation.

In solid mechanics, the linear elasticity field plays an important role. By considering small displacements and linear stress-strain behaviour, the linear elasticity allows the analysis of deformation and stress distribution in elastic materials (Timoshenko and Goodier, 1934). In order to solve linear elasticity problems, the governing equations are expressed in terms of equilibrium equations, kinematic relations and constitutive equations. The equilibrium guarantees that the sum of forces and moments acting on an infinitesimal element is equal to zero. The kinematic relations provide a direct link between strain and displacements. The constitutive equations establish the relationship between stress and strain, providing a description of material behaviour. Linear elasticity facilitates the examination of mechanical properties in a diverse range of engineering materials, encompassing metals, polymers, and composites.

The accurate modelling of such physical and engineering problems requires a rigorous numerical implementation. An adequate discretization in BEM can certainly provide highly precise results. Recently, this method has been improved by the introduction of different shape functions. The Non-Uniform Rational B-splines (NURBS) are used instead of the Lagrangian polynomials, as done in conventional BEM. The NURBS, utilized in Computer-Aided Design (CAD) software, offer convenience in free-form surface modelling and accurately represents various conic sections such as circles, cylinders, spheres, and more (Cottrell *et al.*, 2009). The application of NURBS in numerical modelling has led to the development of Isogeometric Analysis (IGA). Hence, enhanced geometric accuracy and improved solutions are obtained by the application of IGABEM.

Therefore, the present work aims to explore the advantages of IGABEM by analyzing problems considering the potential theory and linear elasticity. Through the utilization of NURBS in the numerical modelling process, IGABEM

harnesses its benefits, providing a promising and effective approach for accurately and efficiently analyzing problems across different fields of study.

2. THE BOUNDARY ELEMENT METHOD (BEM)

The boundary element method (BEM) is commonly employed for solving potential and elastostatic problems. Boundary elements have become a robust alternative to finite elements, especially in situations where enhanced precision is necessary. This is particularly applicable in scenarios involving issues like stress concentration or domains that extend infinitely (Brebbia and Dominguez, 1994). The approach relies on the boundary integral equations of the governing problem, which can be derived from the weighted integral representation of the differential equations of the boundary value problem, utilizing the fundamental solution (Brebbia and Dominguez, 1994; Aliabadi, 2002).

2.1 Boundary integral equations for potential problems

The concept of potential theory allows for the representation of physical phenomena, wherein the gradient of a given variable associated with the problem is restricted by a conservation law. This theory proves highly applicable in a wide range of situations, including heat conduction, fluid diffusion, and the distribution of electric and magnetic charges (Cordeiro and Leonel, 2014).

In order to introduce the potential theory, let's first consider the Laplace equation, which is extensively employed in the fields of science and engineering to model a diverse array of problems, making it one of the most widely utilized partial differential equations (Cheng and Cheng, 2005). The Laplace equation is a particularization of the Poisson equation, which is given by:

$$\nabla^2 \varphi(x,y) = b \tag{1}$$

where $\varphi(x,y)$ is the potential function and b is the domain term. For the Laplace equation, $b = 0$.

The formulation of the potential problem can be performed considering the relation given in Eq. (2), as follows:

$$\varphi(x,y) = \varphi^*_{ij}(x,y)\mu_j \tag{2}$$

in which $\varphi^*_{ij}(x,y)$ is the fundalmental solution of the plane potential problem at the point j due to a concentrated load acting at point i and μ_j is the unknown field at the collocation point j.

In plane potential problems, the fundamental solution is given by:

$$\varphi^*_{ij}(x,y) = \frac{-1}{2\pi}\ln(r) \tag{3}$$

in which r is the distance between the source and the field point.

To address problems where both the potential and flux values q^* can be prescribed, it is necessary to calculate the derivative of Equation (2) with respect to the normal orientation to the boundary, i.e:

$$\frac{\partial \varphi(x,y)}{\partial \eta} = \frac{\partial \varphi^*_{ij}(x,y)}{\partial \eta}\mu_j \tag{4}$$

in which

$$\frac{\partial \varphi^*_{ij}(x,y)}{\partial \eta} = q^*_{ij}(x,y) = \frac{-1}{2\pi r}\frac{\partial r}{\partial \eta} \tag{5}$$

Hence, according to Brebbia and Dominguez (1994), assuming $b = 0$, the integral representation for the Laplace problems is defined as:

$$\mathrm{c}(x')\varphi(x) + \int_\Gamma q^*(x',x)\varphi(x)d\Gamma = \int_\Gamma \varphi^*(x',x)q(x)d\Gamma \tag{6}$$

where x' represents the source point; x the field point, and $c(x')$ represents the free term. The value of $c(x')$ is assumed to be 0 for points outside the domain, 1 for points inside the domain, and $1/2$ for points located on a smooth boundary.

2.2 Boundary integral equations of linear elasticity

The well-known Somigliana's identity, used to determine the displacement at any point within the domain Ω, can be expressed as follows:

$$u_i\left(\mathbf{x}'\right)+\int_\Gamma T_{ij}^*\left(\mathbf{x}',\mathbf{x}\right)u_j(\mathbf{x})d\Gamma=\int_\Gamma U_{ij}^*\left(\mathbf{x}',\mathbf{x}\right)t_j(\mathbf{x})d\Gamma+\int_\Omega U_{ij}^*\left(\mathbf{x}',\mathbf{x}\right)b_j(\mathbf{x})d\Omega \tag{7}$$

where u_i represents the displacements; t_i the tractions; and b_i and the body forces. The superscript $*$ in $\mathbf{T}^*$(**x'**,**x**) and $\mathbf{U}^*$(**x'**,**x**) represents the fundamental solution associated with each field. The fundamental solution takes into account an infinite domain subjected to the influence of a singular load, represented by the Delta Dirac function.

Following the mathematical procedure demonstrated in (Aliabadi, 2002) , the displacement and traction fundamental solutions are defined respectively as:

$$U_{ij}^*\left(\mathbf{x}',\mathbf{x}\right)=\frac{1}{8\pi\mu(1-\nu)}\left[(3-4\nu)\ln\left(\frac{1}{r}\right)\delta_{ij}+r_{,i}r_{,j}\right] \tag{8}$$

$$T_{ij}^*\left(\mathbf{x}',\mathbf{x}\right)=-\frac{1}{4\pi(1-\nu)r}\left\{(1-2\nu)\left(r_{,j}n_i-r_{,i}n_j\right)+r_{,n}\left[(1-2\nu)\delta_{ij}+2r_{,i}r_{,j}\right]\right\} \tag{9}$$

in the above equations, ν is the Poisson coefficient; r is is the distance between the source $\mathbf{x}'$ and the field point $\mathbf{x}$ and n is the normal vector.

To solve the boundary value problem, a limit analysis is performed in Eq. (7), where the source point is taken into the boundary. Hence, the following expression is obtained:

$$C_{ij}u_j\left(\mathbf{x}'\right)+\int_\Gamma T_{ij}^*\left(\mathbf{x}',\mathbf{x}\right)u_j(\mathbf{x})d\Gamma=\int_\Gamma U_{ij}^*\left(\mathbf{x}',\mathbf{x}\right)t_j(\mathbf{x})d\Gamma+\int_\Omega U_{ij}^*\left(\mathbf{x}',\mathbf{x}\right)b_j(\mathbf{x})d\Omega \tag{10}$$

where C_{ij} corresponds to the free term, assuming half of identity operator for smooth boundaries.

To determine the internal stresses field, the Somigliana identity is derived with respect to the source point $\mathbf{x}'$. By incorporating the strain-displacement relation and Hooke's law into the resulting expression, the subsequent integral equation is obtained:

$$\sigma_{ij}\left(\mathbf{x}'\right)+\int_\Gamma S_{kij}^*\left(\mathbf{x}',\mathbf{x}\right)u_k(\mathbf{x})d\Gamma=\int_\Gamma D_{kij}^*\left(\mathbf{x}',\mathbf{x}\right)t_k(\mathbf{x})d\Gamma+\int_\Omega D_{kij}^*\left(\mathbf{x}',\mathbf{x}\right)b_k(\mathbf{x})d\Omega \tag{11}$$

where S_{kij}^* and D_{kij}^* come from the derivative of U_{ij}^* and T_{ij}^* with respect to $\mathbf{x}'$, as presented:

$$D_{kij}^*\left(\mathbf{x}',\mathbf{x}\right)=\frac{1}{4\pi(1-\nu)r}\left[(1-2\nu)\left(r_{,i}\delta_{jk}+r_{,j}\delta_{ik}-r_{,k}\delta_{ij}\right)+2r_{,i}r_{,j}r_{,k}\right] \tag{12}$$

$$\begin{aligned}S_{kij}^*\left(\mathbf{x}',\mathbf{x}\right)=\frac{\mu}{2\pi(1-\nu)r^2}\Bigg\{&2\frac{\partial r}{\partial n}\left[(1-2\nu)r_{,k}\delta_{ij}+\nu\left(r_{,i}\delta_{jk}+r_{,j}\delta_{ik}\right)-4r_{,i}r_{,j}r_{,k}\right]+\\&+2\nu\left(n_ir_{,j}r_{,k}+n_jr_{,i}r_{,k}\right)+(1-2\nu)\left(2n_kr_{,i}r_{,j}+n_i\delta_{jk}+n_j\delta_{ik}\right)-(1-4\nu)n_k\delta_{ij}\Bigg\}\end{aligned} \tag{13}$$

in which δ_{ij} represents the Kronecker delta.

3. NUMERICAL APPROXIMATION

Approximations are required in order to obtain numerical solutions for the relations shown in Eq. (10) and Eq. (11). These equations are evaluated for each element e and each collocation point, as shown in Fig. (1a and 1b). Discontinuous elements are herein considered to solve the discontinuous traction field problems, as typically done in a BEM analysis. In this study, the endpoints exhibit discontinuity at intervals of one-fourth the total length of the element. As also presented in Fig. (1b), these elements can be linear, quadratic, cubic, and so on. Thus, the geometry as well as the mechanical fields can be approximated by the following:

$$\mathbf{x}^e = \sum_{\alpha=1}^{m} N_\alpha(\xi)\mathbf{x}_\alpha \tag{14}$$

$$\mathbf{u}^e = \sum_{\alpha=1}^{m} N_\alpha(\xi)\mathbf{u}_\alpha \tag{15}$$

$$\mathbf{t}^e = \sum_{\alpha=1}^{m} N_\alpha(\xi)\mathbf{t}_\alpha \tag{16}$$

where $\mathbf{x}_\alpha$, $\mathbf{u}_\alpha$ and $\mathbf{t}_\alpha$ are the values of the functions at node α and N_α represents the shape functions defined in terms of non-dimensional coordinates ξ $(-1 \leq \xi \leq 1)$. In the conventional Boundary Element Method (BEM), these shape functions are Lagrangian polynomials, while in Isogeometric Analysis Boundary Element Method (IGABEM), they are Non-Uniform Rational B-splines (NURBS). More comprehensive discussions on these shape functions will be provided in the following sections.

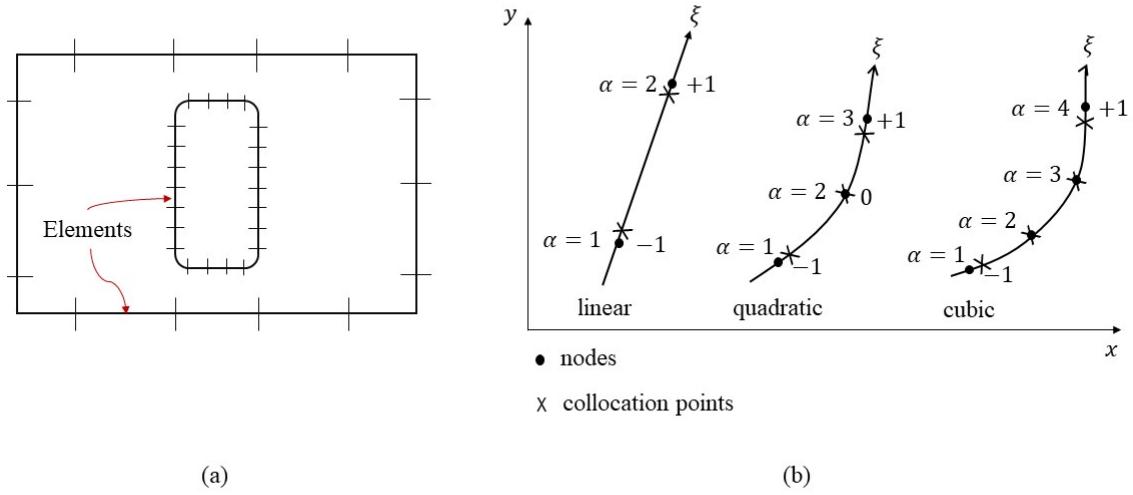

Figure 1. (a) Discretization of the boundary into elements and (b) their representation in the isoparametric space.
Source: Adapted from Aliabadi (2002).

By disregarding the presence of the body forces and by discretizing the problem into N elements, Eq. (10) leads to the following:

$$C_{ij}\left(\mathbf{x}'\right) u_j\left(\mathbf{x}'\right) + \sum_{n=1}^{N_e} \int_{\Gamma_n} T_{ij}^*\left(\mathbf{x}', \mathbf{x}\right) u_j(\mathbf{x}) d\Gamma = \sum_{n=1}^{N_e} \int_{\Gamma_n} U_{ij}^*\left(\mathbf{x}', \mathbf{x}\right) t_j(\mathbf{x}) d\Gamma \tag{17}$$

where $\Gamma = \sum_{n=1}^{N} \Gamma_n$. The kernels $\mathbf{T}^*$(**x'**,**x**) and $\mathbf{U}^*$(**x'**,**x**) are computed in a matrix form for every integration point, as follows:

$$\boldsymbol{T}^* = \begin{bmatrix} t_{11}^* & t_{12}^* \\ t_{21}^* & t_{22}^* \end{bmatrix} \tag{18}$$

$$\boldsymbol{U}^* = \begin{bmatrix} u_{11}^* & u_{12}^* \\ u_{21}^* & u_{22}^* \end{bmatrix} \tag{19}$$

where the subindices i and j of t_{ij} and u_{ij} are the resulting tractions and displacements, respectively, in j direction due to the application of a unitary force in i direction.

By substituting the expressions given in Eqs. (14)-(16) into the integral equation (17), one obtains

$$C_{ij}\left(\mathbf{x}'\right)u_j\left(\mathbf{x}'\right)+\sum_{n=1}^{N}\sum_{\alpha=1}^{m}DH_{ij}^{n\alpha}u_j^{n\alpha}=\sum_{n=1}^{N}\sum_{\alpha=1}^{m}DG_{ij}^{n\alpha}t_j^{n\alpha}\quad i,j=1,2 \tag{20}$$

where

$$DH_{ij}^{n\alpha}=\int_{-1}^{1}N_\alpha(\xi)T_{ij}^{*}\left[\mathbf{x}',\mathbf{x}(\xi)\right]J^n(\xi)d\xi \tag{21}$$

$$DG_{ij}^{n\alpha}=\int_{-1}^{1}N_\alpha(\xi)U_{ij}^{*}\left[\mathbf{x}',\mathbf{x}(\xi)\right]J^n(\xi)d\xi \tag{22}$$

in which the Jacobian of transformation $J(\xi)$ is given by

$$J(\xi)=\sqrt{\left(\frac{dx_1}{d\xi}\right)^2+\left(\frac{dx_2}{d\xi}\right)^2} \tag{23}$$

The regular integrals are performed with standard Gaussian quadrature, while the singular integrations are treated by means of the subtraction singularity technique, as detailed in Brebbia and Dominguez (1994). The BEM usual system of equations for solving Eq. (7) is then assembled:

$$\mathbf{Hu}=\mathbf{Gt} \tag{24}$$

where the square matrix **H** contains all the integrals of the T^*(**x'**,**x**) kernel and **G** of the U^*(**x'**,**x**) one; **u** and **t** are the vectors that contain the nodal displacements and the tractions.

After prescribing the boundary conditions, Eq. (24) is reorganized into the subsequent system:

$$\mathbf{Ax}=\mathbf{f} \tag{25}$$

where **x** corresponds to the vector of unknown degrees of freedom and **A** is a full and non-symmetric matrix.

3.1 Conventional BEM

The main difference between the conventional BEM and the IGABEM lies in the definition of the shape functions. In conventional BEM analysis, the shape functions N_α are obtained from Lagrangian polynomials, as given below:

$$N_i(\xi)=\prod_{i=1,i\neq j}^{m}\frac{\xi-\xi_j}{\xi_i-\xi_j} \tag{26}$$

where its degree is $m-1$, in which m is the total number of nodes, and they assume the value 1 at node α and zero at all other nodes. The sum of all shape functions must be equal to 1 while the sum of its first derivative assumes the value of zero.

The first-order derivatives of Eq. (27) provide the tangent and normal vectors, as well as the Jacobian of transformation. These derivatives can be expressed using the following equation:

$$N_{i,\xi}(\xi)=\sum_{i=1,i\neq j}^{m}\prod_{i=1,j\neq i,k\neq i,k\neq j}^{m}\frac{1}{\xi_i-\xi_j}\frac{\xi-\xi_k}{\xi_i-\xi_k} \tag{27}$$

3.2 The isogeometric boundary element method (IGABEM)

To understand the concept of NURBS, one must first consider the basis splines, also known as b-splines. For defining such curves, it is of primary importance to know three basic characteristics:

- Control points;
- Knot vectors;
- Order of approximation.

Drawing from the concepts presented in the works of Cottrell et al. (2009), Simpson (2012, 2013), the shape of a curve is defined by a set of control points. Additionally, the knot vectors, which consist of a non-decreasing sequence of coordinates in the parametric space denoted as $\Xi = \{\xi_1, \xi_2, \ldots, \xi_{n+p+1}\}$, play a crucial role. In this context, the knot index is represented by i, ξ_i signifies the i^{th} knot, p corresponds to the polynomial order, and n represents the number of basis functions employed to construct the B-spline functions.

In the present work, the knot spans are considered elements once the numerical quadrature is carried out at the knot span level. The knot spans are the intervals between each parametric coordinate of a defined knot vector. Hence, the basis functions are defined recursively starting with piecewise constants, as follows for $p = 0$, with $1 \leq a \leq n$:

$$N_{a,0} = \begin{cases} 1 & \text{if } \xi_a \leq \xi < \xi_{a+1} \\ 0 & \text{otherwise} \end{cases} \tag{28}$$

For $p = 1, 2, 3...$, the recursive Cox-de Boor formula (Cox, 1972; De Boor, 1972) is used:

$$N_{i,p}(\xi) = \frac{\xi - \xi_i}{\xi_{i+p} - \xi_i} N_{i,p-1}(\xi) + \frac{\xi_{i+p+1} - \xi}{\xi_{i+p+1} - \xi_{i+1}} N_{i+1,p-1}(\xi) \tag{29}$$

The first-order derivatives of a B-spline function can be obtained through:

$$\frac{d}{d\xi} N_{i,p}(\xi) = \frac{p}{\xi_{i+p} - \xi_i} N_{i,p-1}(\xi) - \frac{p}{\xi_{i+p+1} - \xi_{i+1}} N_{i+1,p-1}(\xi) \tag{30}$$

Although B-splines are only capable of approximating circular shapes, NURBS (Non-Uniform Rational B-Splines) have the ability to precisely reproduce them (Simpson *et al.*, 2013). This is achieved by generating these functions through a projection of B-splines and introducing an additional coordinate known as weight w. The interpolation using NURBS can be expressed as follows:

$$\mathbf{c}(\xi) = \sum_{a=1}^{n} R_{a,p}(\xi) \mathbf{p}_a \tag{31}$$

where p_a stands for the control points and $R_{a,p}$ is given by

$$R_{a,p} = \frac{N_{a,p}(\xi) w_a}{\sum_{\hat{a}=1}^{m} N_{\hat{a},p}(\xi) w_{\hat{a}}} \tag{32}$$

The first-order derivatives of the NURBS are obtained by:

$$\frac{d}{d\xi} R_{a,p}(\xi) = w_a \frac{W(\xi) N'_{a,p} - W'(\xi) N_{a,p}(\xi)}{W(\xi)^2} \tag{33}$$

in which

$$W(\xi) = \sum_{\hat{a}=1}^{n} N_{\hat{a},p}(\xi) w_a, \tag{34}$$

$$N'_{a,p} \equiv \frac{d}{d\xi} N_{a,p} \tag{35}$$

and

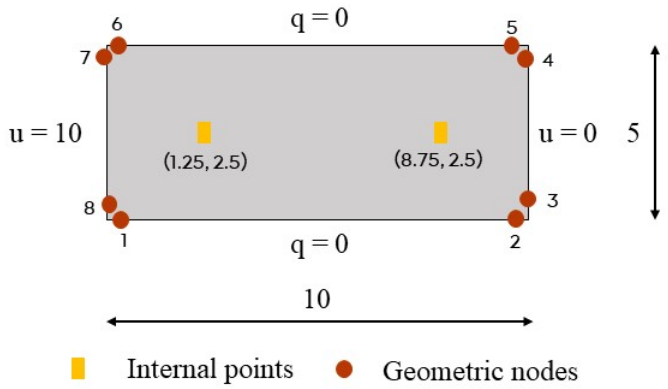

Figure 2. Problem addressing a linear variation of the potential.

$$W'(\xi) = \sum_{\hat{a}=1}^{n} N'_{\hat{a},p}(\xi) w_a. \tag{36}$$

For the numerical implementation of the problem, once the integration is carried out into the knot spans and not directly in the NURB, an additional transformation Jacobian must be considered. In a knot span $[\xi_1, \xi_2]$, for example, the parametric coordinate is defined according to:

$$\xi = \frac{(\xi_2 - \xi_1)\,\hat{\xi} + (\xi_2 + \xi_1)}{2} \tag{37}$$

where $\hat{\xi}$ is the Gauss coordinate. Hence, the Jacobian is given by:

$$\frac{\partial \xi}{\partial \hat{\xi}} = \frac{\xi_2 - \xi_1}{2} \tag{38}$$

4. NUMERICAL EXAMPLES

In this section, the BEM and IGABEM analyses are compared using three numerical examples implemented in FORTRAN 90 code. The first subsection focuses on applying the boundary integral equations for potential problems, as developed in section 2.1. Two examples are presented within this subsection. The second subsection addresses the application of boundary integrals, as explained in section 2.2, for solving elastostatics problems. An additional example is provided. The results are compared, and the most accurate outcomes are highlighted.

4.1 Potential theory applications

4.1.1 Linear variation of the potential

Let's start by considering a basic example involving a linear variation of the potential. As illustrated in Fig. (2), the potential values are specified as $u = 10$ on the left side, gradually decreasing linearly until it reaches $u = 0$ on the right side. Furthermore, the fluxes at both the bottom and top are known to be equal, with a value of $q = 0$.

To perform the BEM analysis, the geometry is discretized using 4 linear elements, resulting in a total of 8 geometric nodes. In order to perform the numerical integration, 150 integration points are considered in each element. On the other hand, for the IGABEM analysis, 4 NURBS are considered, with each curve having two control points of weight $w = 1$. The results of each analysis are contrasted in Tab. 1.

The potential and flux values are evaluated for two internal points, as also shown in Fig. (2). The results are compared in Tab. 2. As can be noted, both analyses yield identical solutions. This is expected once linear elements are considered, in which the Lagrangian polynomials approximate both geometry and mechanical fields without losing precision.

4.1.2 Circular domain with a hole

The second example is given in de Barros Souza (2021) and it refers to a circular domain containing a hole with an internal radius equal to a and an external radius b. The boundary conditions are presented in Fig. 3, where the adopted

Table 1. Comparison between the BEM and IGABEM analysis for a linear variation of the potential.

Node ID	Potential value (BEM)	Potential value (IGABEM)	Flux value (BEM)	Flux value (IGABEM)
1	7.49999	7.49999	0.0	0.0
2	2.5	2.49999	0.0	0.0
3	0.0	0.0	-0.99999	-1.0
4	0.0	0.0	-1.0	-0.99999
5	2.5	2.5	0.0	0.0
6	7.5	7.5	0.0	0.0
7	10.0	10.0	1.0	1.0
8	10.0	10.0	0.99999	0.99999

Table 2. Comparison between the BEM and IGABEM analysis for the selected internal points.

Coordinates	Potential value (BEM)	Potential value (IGABEM)	Flux value (BEM)	Flux value (IGABEM)
(1.25, 2.5)	8.75	8.75	-1.0	-1.0
(8.75, 2.5)	1.25	1.25	-1.0	-1.0

theoretical values are: $a = 1$, $b = 2$, $u_a = 100$ and $q_b = 200$.

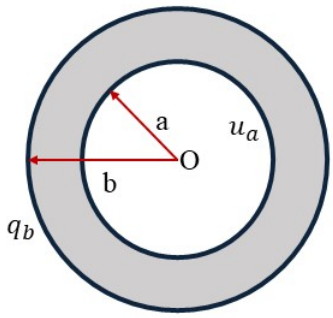

Figure 3. Circular domain with a hole with prescribed boundary conditions u_a and q_b.

The problem presents an analytical solution given in Liu and Nishimura (2006), according to the following expressions:

$$u(r) = u_a + q_b b \ln\left(\frac{r}{a}\right) \tag{39}$$

$$q(r) = -q_b \frac{b}{r} \tag{40}$$

in which r is the radius.

Evaluating Eqs. (39) and (40) at the midpoint of the domain, i.e, at $r = 1.5$, $u(1.5) = 262.186$ and $q(1.5) = -266.666$. In the BEM analysis, the numerical approximation involves 16 quadratic elements (2 in each quadrant), resulting in a total of 48 collocation points. On the other hand, the IGABEM analysis utilizes 8 NURBS curves (1 in each quadrant) described by 3 control points each, yielding an approximation of $p = 2$. Hence, only 24 collocation points are used. The knot vectors are equal to $\Xi = [0, 0, 0, 1, 1, 1]$. The weights related to each control point are $w = [1, 0.70710678, 1]$.

The numerical values of both approximations are given in Tab. 3. Figure 4 illustrates the variation of the potential values on the external boundary. Note that a variable s is considered. The variable goes through the perimeter of the structural element, starting at $s = 0$ and ending at $s = 12.566$. As can be observed, the IGABEM analysis provides a more accurate solution when compared to the analytical response. This outcome is expected since the employed shape functions of order 2 precisely represent the geometry.

Table 3. Comparison between the BEM and IGABEM at the midpoint $r = 1.5$.

$\mathbf{u(r)}$ **(BEM)**	$\mathbf{u(r)}$ **(IGABEM)**	$\mathbf{q(r)}$ **(BEM)**	$\mathbf{q(r)}$ **(IGABEM)**
262.28863	262.18734	-266.50073	-266.66687

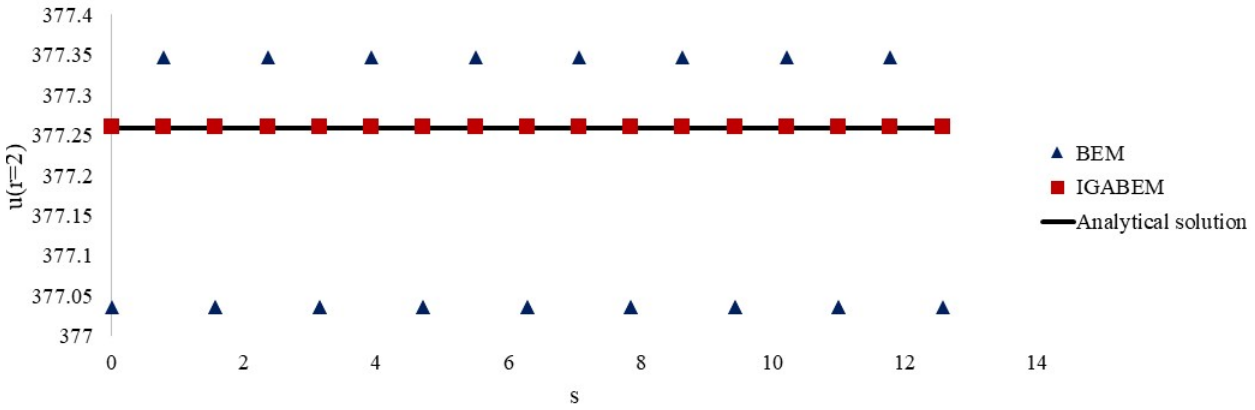

Figure 4. Comparison of the potential variation on the external boundary.

4.2 Elastotastics applications

The example proposed in this case is an infinite plate with a circular hole subjected to constant traction $T_x = 10kN/m^2$. The analytical solution for this problem is available in Gould and Feng (1994). Figure (5) illustrates the problem. Here, for the geometry discretization, the plate length L is chosen to be a substantially larger value than the radius of the cavity, which is denoted as r. A value of $r = 5m$ is considered for the radius, which is 100 times smaller than the length L of $500m$. The material properties are: $E = 100MPa$ and $\nu = 0.3$.

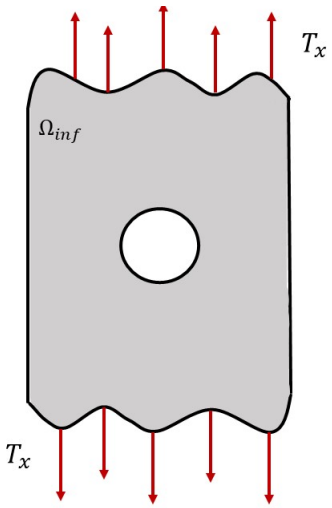

Figure 5. Representation of an infinite plate with a small circular hole.

In the BEM analysis, a total of 12 quadratic elements are considered, out of which 8 are utilized to describe the hole, totaling 36 collocation points. This involves assigning 2 quadratic elements per quadrant. In contrast, the IGABEM analysis only necessitates 8 NURBS, with a single quadratic NURB per quadrant being sufficient to describe the hole. A total of 20 collocation points is used.

Through the IGABEM analysis, Fig. (6) displays the stress field in x direction. Note that there is a stress concentration at the edge of the hole. This is expected because St. Venant's Principle predicts that the stress distribution is modified solely in the proximity of the hole, while it remains constant in the rest of the domain. Furthermore, note that the value tends to $\sigma_x = 3T_x$ as it gets closer to the hole's edge. This result is in accordance with the analytical solution of the problem, where the value of 3 is the well-known stress concentration factor K. This factor measures the ratio of the

maximum stress at a point in a material to the nominal stress that is applied to the material.

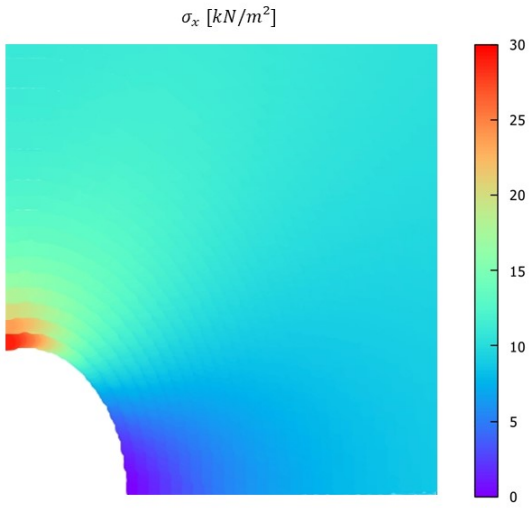

Figure 6. Stress field in x direction.

The numerical value obtained at the edge of the hole in IGABEM equals $30.20891 kN/m^2$. Analyzing this problem through conventional BEM requires more computational effort since additional elements are needed. The response obtained via BEM is $32.09914 kN/m^2$, indicating a tendency towards the analytical solution. However, it still exhibits a more significant error compared to IGABEM.

5. SUMMARY AND CONCLUSIONS

The numerical examples presented have highlighted the advantages and potential of IGABEM analysis compared to conventional BEM. For instance, IGABEM effectively addresses the distribution of physical fields and their interactions with boundaries by solving the governing equations derived from the potential theory. This theory finds wide applications in diverse problem domains, including fluid dynamics, electromagnetics, and structural analysis. The governing equations derived from the linear elasticity also present the capability of IGABEM to model and analyze the stress distribution in elastic materials.

Although IGABEM is a relatively new numerical tool, it is being largely used due to its capacity to accurately approximate both geometry and mechanical field. By a projection of the B-splines, IGA utilizes the NURBS as basis and shape functions. The integration of geometry and analysis leads to a more efficient process. This allows a more accurate representation of complex geometries compared to conventional BEM, which typically relies on piecewise linear or quadratic elements. Further research and development continue to refine and improve IGABEM applications. Its potential for addressing even broader problems is increasingly evident.

6. ACKNOWLEDGEMENTS

Sponsorship of this research project by the São Paulo State Foundation for Research (FAPESP), Brazil, project number 2022/03377-7, is greatly appreciated.

7. REFERENCES

Aliabadi, M.H., 2002. *The boundary element method, volume 2: applications in solids and structures*, Vol. 2. John Wiley & Sons.

Brebbia, C.A. and Dominguez, J., 1994. *Boundary elements: an introductory course*. WIT press.

Cheng, A.H.D. and Cheng, D.T., 2005. "Heritage and early history of the boundary element method". *Engineering analysis with boundary elements*, Vol. 29, No. 3, pp. 268–302.

Cordeiro, S.G.F. and Leonel, E.D., 2014. "Análise de problemas de potencial por meio do método das soluções fundamentais e do método dos elementos de contorno com reciprocidade dual e elementos de alta ordem".

Cottrell, J.A., Hughes, T.J. and Bazilevs, Y., 2009. *Isogeometric analysis: toward integration of CAD and FEA*. John Wiley & Sons.

Cox, M.G., 1972. "The numerical evaluation of b-splines". *IMA Journal of Applied mathematics*, Vol. 10, No. 2, pp. 134–149.

de Barros Souza, V., 2021. *Formulações numéricas baseadas no Método dos Elementos de Contorno para a análise probabilística da difusão de cloretos no concreto*. Master's thesis, Universidade de São Paulo.

De Boor, C., 1972. "On calculating with b-splines". *Journal of Approximation theory*, Vol. 6, No. 1, pp. 50–62.

Gould, P.L. and Feng, Y., 1994. *Introduction to linear elasticity*. Springer.

Kellogg, O.D., 1953. *Foundations of potential theory*, Vol. 31. Courier Corporation.

Liu, Y. and Nishimura, N., 2006. "The fast multipole boundary element method for potential problems: a tutorial". *Engineering Analysis with Boundary Elements*, Vol. 30, No. 5, pp. 371–381.

Simpson, R.N., Bordas, S.P., Lian, H. and Trevelyan, J., 2013. "An isogeometric boundary element method for elastostatic analysis: 2d implementation aspects". *Computers & Structures*, Vol. 118, pp. 2–12.

Timoshenko, S. and Goodier, J., 1934. *Theory of elasticity. New York and London*. McGraw-Hill Book.

8. RESPONSIBILITY NOTICE

The following text, properly adapted to the number of authors, must be included in the last section of the paper: The author(s) is (are) solely responsible for the printed material included in this paper.